



Pharmaceutical Nanotechnology

Idebenone-loaded solid lipid nanoparticles for drug delivery to the skin: *In vitro* evaluationLucia Montenegro^{a,*}, Chiara Sinico^b, Ines Castangia^b, Claudia Carbone^a, Giovanni Puglisi^a^a Department of Drug Sciences, University of Catania, V.le A. Doria, 6, 95125 Catania, Italy^b Department of Life and Environment Sciences, Via Ospedale 72, 09124 Cagliari, Italy

ARTICLE INFO

Article history:

Received 2 April 2012

Received in revised form 21 May 2012

Accepted 21 May 2012

Available online 29 May 2012

Keywords:

Idebenone

Skin permeation

Skin penetration

Solid lipid nanoparticles

Skin delivery

ABSTRACT

Idebenone (IDE), a synthetic derivative of ubiquinone, shows a potent antioxidant activity that could be beneficial in the treatment of skin oxidative damages. In this work, the feasibility of targeting IDE into the upper layers of the skin by topical application of IDE-loaded solid lipid nanoparticles (SLN) was evaluated. SLN loading different amounts of IDE were prepared by the phase inversion temperature method using cetyl palmitate as solid lipid and three different non-ionic surfactants: ceteth-20, isoceteth-20 and oleth-20. All IDE loaded SLN showed a mean particle size in the range of 30–49 nm and a single peak in size distribution. *In vitro* permeation/penetration experiments were performed on pig skin using Franz-type diffusion cells. IDE penetration into the different skin layers depended on the type of SLN used while no IDE permeation occurred from all the SLN under investigation. The highest IDE content was found in the epidermis when SLN contained ceteth-20 or isoceteth-20 as surfactant while IDE distribution into the upper skin layers depended on the amount of IDE loaded when oleth-20 was used as surfactant. These results suggest that the SLN tested could be an interesting carrier for IDE targeting to the upper skin layers.

© 2012 Elsevier B.V. All rights reserved.

1. Introduction

In recent years, great interest has been focused on the use of antioxidants for topical administration. Being the outermost barrier of the body, the skin is exposed to various exogenous sources of oxidative stress, including ultraviolet radiation and pollutants. As response to these oxidative attacks, reactive oxygen species (ROS) and other free radicals are generated in the skin (Dreher and Maibach, 2001). To counteract the deleterious effects of ROS, an antioxidant network consisting of a variety of lipophilic (e.g. vitamin E, ubiquinones, carotenoids) and hydrophilic (e.g. vitamin C, uric acid and glutathione) antioxidants is present in the skin and is responsible for the balance between pro-oxidants and antioxidant (Thiele et al., 2000). An impairment of this balance, due to an increased exposure to exogenous sources of ROS, has been defined as “oxidative stress” and involves oxidative damages of lipids, proteins and DNA (Sies, 1985). Generally, the epidermis contains higher concentrations of antioxidants compared to the dermis while the horny layer lacks of co-antioxidants such as ubiquinol 10 that, on the contrary, is the most abundant ubiquinone contained in human skin. Topical administration of antioxidants is regarded as an interesting strategy in reducing ROS induced skin

damages since it may improve skin antioxidant capacity (Dreher and Maibach, 2001). A topical supplementation with antioxidants could be particularly beneficial for the stratum corneum due to its high susceptibility for UV and ozone-induced depletion of antioxidants (Thiele et al., 1998).

In the last decades, many colloidal carriers have been proposed for drug targeting to the skin, such as liposomes (Bernard et al., 1997; Mezei et al., 1994) and solid lipid nanoparticles (SLN) (Papakostas et al., 2011; Pardeike et al., 2009; Zhang and Smith, 2011). The latter show several advantages compared to other drug delivery systems: good local tolerability, improved drug stability, drug targeting, increased bioavailability, ability to incorporate drugs with different physico-chemical properties, high inclusion rate for lipophilic substances and small particle size allowing close contact to the stratum corneum (Müller et al., 2000; Mehnert and Mäeder, 2001).

Recently, we have developed a novel technique to prepare SLN using low amounts of surfactants by means of the phase inversion temperature (PIT) method, that allowed us to obtain SLN with promising physico-chemical and technological properties such as good stability, small particle size, narrow size distribution and good loading capacity (Montenegro et al., 2011, 2012). Such SLN were loaded with idebenone (IDE, Fig. 1), a synthetic derivative of ubiquinone with a shorter carbon side chain and a subsequent increased solubility (Wieland et al., 1995). IDE anti-oxidant activity is due to its structural analogy with coenzyme Q₁₀, a natural

* Corresponding author. Tel.: +39 095 738 40 10; fax: +39 095 738 42 11.
E-mail address: lmontene@unict.it (L. Montenegro).

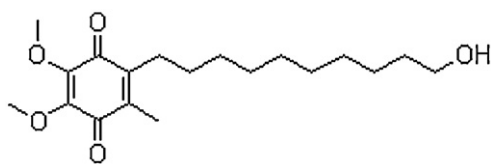


Fig. 1. Chemical structure of IDE.

antioxidant of cell membranes involved in the mitochondrial electronic transport chain (Crane, 2001; Dallner and Sindelar, 2000). IDE potent antioxidant activity has been mainly attributed to its ability to inhibit lipid peroxidation (LPO), and to protect cell and mitochondrial membranes from oxidative damage (Imada et al., 1989). IDE antioxidant activity has been proposed to be beneficial in preventing skin aging and to protect the skin from oxidative damages due to its exposure to environmental oxidative agents (Hoppe et al., 1999), other than in the treatment of neurodegenerative diseases (Schols et al., 2004).

In recent years, nanostructured lipid carriers have been reported to be effective in increasing skin permeation of Coenzyme Q₁₀ (Junyaprasert et al., 2009) and of idebenone (Li and Ge, 2012), thus suggesting that nanoparticles containing these antioxidants could have significant potential use as topical formulations for reducing skin oxidative damages.

Therefore, in this work we assessed the feasibility of targeting IDE into the upper layers of the skin (stratum corneum and epidermis) by topical application of IDE-loaded SLN prepared by the PIT method. With this aim, *in vitro* permeation and penetration studies were performed on newborn pig skin using SLN loaded with different amounts of IDE, consisting of cetyl palmitate as lipid core and various non-ionic surfactants. IDE loaded SLN investigated in this paper had a composition similar to that of IDE loaded SLN described for drug delivery to the brain (Montenegro et al., 2011, 2012). Cetyl palmitate was chosen as solid lipid because of its good tolerability both after topical and systemic administration (Wang et al., 2009; Lukowski et al., 2000). After *in vitro* application on the skin surface of IDE-loaded SLN, IDE penetration into the different skin layers together with its permeation through the skin were evaluated.

2. Materials and methods

2.1. Materials

Polyoxyethylene-20-cetyl ether (Brij 58[®], Ceteth-20) was supplied by Fluka (Milan, Italy). Polyoxyethylene-20-isohexadecyl ether (Arlasolve 200 L[®], Isoceteth-20) was a kind gift of Bregaglio (Milan, Italy). Polyoxyethylene-20-oleyl ether (Brij 98[®], Oleth-20, was bought from Sigma–Aldrich (Milan, Italy). Glyceryl oleate (Tegin O[®], GO) was obtained from Th. Goldschmidt Ag (Milan, Italy). Cetyl Palmitate (Cutina CP[®], CP) was purchased from Cognis S.p.a. Care Chemicals (Como, Italy). Idebenone (IDE) was a kind gift of Wyeth Lederle (Catania, Italy). Methylchloroisothiazolinone and methylisothiazolinone (Kathon CG[®]), and imidazolidinyl urea were kindly supplied by Sinerga (Milan, Italy). Poloxamer 188 (Lutrol[®] F68) was a gift of BASF (Ludwigshafen, Germany). Regenerated cellulose membranes (Spectra/Por CE; Mol. Wt. Cut off 3000) were supplied by Spectrum (Los Angeles, CA, USA). Methanol and water used in the HPLC procedures were of LC grade and were bought from Merck (Darmstadt, Germany). All other reagents were of analytical grade and used as supplied.

2.2. Preparation of SLN

IDE-loaded SLN, whose composition is reported in Table 1, were prepared using the phase inversion temperature (PIT) method, as

Table 1
Composition (% w/w) of IDE-loaded SLN.

SLN	Ceteth	Isoceteth	Oleth	GO	CP	IDE	Water ^a
C1	8.7	–	–	4.4	7.0	0.5	q b 100
C2	8.7	–	–	4.4	7.0	0.7	q b 100
C3	8.7	–	–	4.4	7.0	1.1	q b 100
I1	–	10.6	–	3.5	7.0	0.5	q b 100
I2	–	10.6	–	3.5	7.0	0.7	q b 100
O1	–	–	7.5	3.7	7.0	0.5	q b 100
O2	–	–	7.5	3.7	7.0	0.7	q b 100
O3	–	–	7.5	3.7	7.0	1.1	q b 100

^a Water containing 0.35% (w/w) imidazolidinyl urea and 0.05% (w/w) Kathon CG.

previously reported (Montenegro et al., 2011). Briefly, the aqueous phase and the oil phase (cetyl palmitate, the selected emulsifiers and different percentages w/w of IDE) were separately heated at ~90 °C; then the aqueous phase was added drop by drop, at constant temperature and under agitation, to the oil phase. The mixture was then cooled to room temperature under slow and continuous stirring. At the phase inversion temperature (PIT), the turbid mixture turned into clear. PIT values were determined using a conductivity meter mod. 525 (Crison, Modena, Italy) which measured an electric conductivity change when the phase inversion from a W/O to an O/W system occurred. Water contained 0.35% (w/w) imidazolidinyl urea and 0.05% (w/w) methylchloroisothiazolinone and methylisothiazolinone as preservatives. A TLC analysis confirmed that no degradation of IDE occurred under these conditions.

2.3. Transmission electron microscopy (TEM)

For negative-staining electron microscopy, 5 µl of SLN dispersions were placed on a 200-mesh formvar copper grid (TAAB Laboratories Equipment, Berks, UK), and allowed to be adsorbed. Then the surplus was removed by filter paper. A drop of 2% (w/v) aqueous solution of uranyl acetate was added over 2 min. After the removal of the surplus, the sample was dried at room condition before imaging the SLN with a transmission electron microscope (model JEM 2010, Jeol, Peabody, MA, USA) operating at an acceleration voltage of 200 kV.

2.4. Photon correlation spectroscopy (PCS)

SLN particle sizes were determined at room temperature using a Zetamaster S (Malvern Instruments, Malvern, UK), by scattering light at 90°. The instrument performed particle sizing by means of a 4 mW laser diode operating at 670 nm. The values of the mean diameter and polydispersity index were the averages of results obtained for three replicates of two separate preparations.

2.5. Differential scanning calorimetry (DSC) analyses

DSC analyses were performed using a Mettler TA STAR^e System equipped with a DSC 822^e cell and a Mettler STAR^e V8.10 software. The reference pan was filled with 100 µl of water containing 0.35% (w/w) imidazolidinyl urea and 0.05% (w/w) methylchloroisothiazolinone and methylisothiazolinone. Indium and palmitic acid (purity ≥99.95% and ≥99.5%, respectively; Fluka, Switzerland) were used to calibrate the calorimetric system in transition temperature and enthalpy changes, following the procedure of the Mettler STAR^e software. 100 µl of each SLN sample (unloaded SLN prepared using the same procedures but without the addition of IDE) was transferred into a 160 µl calorimetric pan, hermetically sealed and submitted to DSC analysis as follows: (i) a heating scan from 5 to 65 °C, at the rate of 2 °C/min; (ii) a cooling scan from 65 to 5 °C, at the rate of 4 °C/min, for at least three times. Each experiment was carried out in triplicate.

2.6. Stability tests

Samples of SLN were stored in airtight jars, and then kept in the dark at room temperature and at 37 °C for two months, separately.

Particle size and polydispersity index of the samples were measured at fixed time intervals (24 h, one week, two weeks, three weeks, one month, and two months) after their preparation.

2.7. Determination of IDE solubility

IDE water solubility was determined in triplicate by stirring an excess of drug in 2 ml of solvent with a magnetic stirrer for 24 h at room temperature and avoiding light exposure to prevent IDE photo-degradation. Thereafter, the mixture was filtered and IDE concentration in its saturated solution was determined by the HPLC method described below.

2.8. In vitro release experiments

IDE release rates from the SLN under investigation were measured through regenerated cellulose membranes using Franz-type diffusion cells (LGA, Berkeley, CA, USA). As reported in the literature (Shah et al., 1989), this technique is regarded as a suitable method for evaluating drug release from pharmaceutical topical formulations.

The cellulose membranes were moistened by immersion in water for 1 h at room temperature before being mounted in Franz-type diffusion cells. Diffusion surface area and receiving chamber volume of the cells were, respectively, 0.75 cm² and 4.5 ml. The receptor was filled with water/ethanol (50/50, v/v) for ensuring pseudo-sink conditions by increasing active compound solubility in the receiving phase. This receiving phase has already been used for *in vitro* release studies of IDE from SLN and no sign of nanoparticle integrity change was observed (Montenegro et al., 2011). The receiving solution was constantly stirred and thermostated at 35 °C to maintain the membrane surface at 32 °C. 200 µl of each formulation was applied on the membrane surface under non occlusion conditions and the experiments were run for 24 h. Due to IDE photostability, all the release experiments were carried out sheltered from the light. At intervals, 200 µl of the receptor phase were withdrawn and replaced with an equal volume of receiving solution pre-equilibrated to 35 °C. The receptor phase samples were analyzed by the HPLC method described below to determine IDE content. At the end of the experiments, samples of the SLN applied on the membrane surface were withdrawn and analyzed to determine particle sizes and polydispersity indexes. Each experiment was performed in triplicate.

2.9. In vitro skin permeation/penetration experiments

Experiments were performed in triplicate (at least five times in order to achieve statistical significance), non-occlusively by means of Franz diffusion vertical cells with an effective diffusion area of 0.785 cm² and skin fragments excised from new born pigs. The subcutaneous fat was carefully removed and the skin was cut into squares of 3 cm × 3 cm and randomized. Goland–Pietrain hybrid pigs (~1.2–1.5 kg), died by natural causes, were provided by a local slaughterhouse. The skin, stored at –80 °C, was pre-equilibrated in physiological solution (NaCl 0.9%, w/v) at 25 °C, 2 h before the experiments. Skin specimens were sandwiched securely between donor and receptor compartments of the Franz cells, with the stratum corneum (SC) side facing the donor compartment. The receptor compartment was filled with 5.5 ml of a 5% Poloxamer 188 water solution, which was continuously stirred with a small magnetic bar. A receptor fluid different from that reported for *in vitro* release experiments was used because a receiving phase consisting of

water/ethanol (50/50, v/v) could damage the barrier integrity of animal skin in *in vitro* skin permeation experiments (Friend, 1992). Due to a slightly different design of Franz-cells used to perform *in vitro* skin permeation experiments, to reach the physiological skin temperature (*i.e.* 32 ± 1 °C) the thermostating bath temperature was set at 37 ± 1 °C throughout the experiments. 200 µl of the tested samples was placed onto the skin surface. The receiving solution was withdrawn after elapsed times of 1, 2, 4, 6, 8 and 24 h, replaced with an equal volume of solution to ensure sink conditions and analyzed by HPLC for drug content.

After 24 h, the skin surface of specimens was washed and the SC was removed by stripping with adhesive tape Tesa® AG (Hamburg, Germany). Each piece of the adhesive tape was firmly pressed on the skin surface and rapidly pulled off with one fluent stroke. The epidermis was separated from the dermis with a surgical sterile scalpel. Tape strips, epidermis, and dermis were placed each in methanol, sonicated to extract the drug and then assayed for drug content by HPLC.

Results were expressed as cumulative amount of IDE penetrated into the different skin layers after 24 h. Mean values ± standard deviation (SD) were calculated and Student's *t*-test was used to evaluate the significance of the difference between mean values. Values of *p* < 0.05 were considered statistically significant.

2.10. High performance liquid chromatography (HPLC) analysis

The HPLC apparatus consisted of a Hewlett-Packard model 1050 liquid chromatograph (Hewlett-Packard, Milan, Italy), equipped with a 20 µl Rheodyne model 7125 injection valve (Rheodyne, Cotati, CA, USA) and an UV-VIS detector (Hewlett-Packard, Milan, Italy).

The chromatographic analyses were performed using a Symmetry, 4.6 cm × 15 cm reverse phase column (C₁₈) (Waters, Milan, Italy) at room temperature and a mobile phase consisting of a methanol/water mixture (80:20, v/v). The column effluent (flow rate 1 ml/min) was monitored continuously at 280 nm to detect IDE. Quantifying IDE was performed by measuring the peak areas in relation to those of a standard calibration curve that was built up by relating known concentrations of IDE with the respective peak areas. No interference of the other formulation components was observed. The sensitivity of the HPLC method was 0.1 µg/ml.

3. Results and discussion

3.1. SLN characterization and stability

IDE-loaded SLN physico-chemical properties were similar to those previously reported (Montenegro et al., 2011). As shown in Fig. 2, transmission electron microscopy (TEM) analyses of the SLN under investigation showed spherical particles with no evident sign of aggregation. As all the images obtained from the SLN under investigation were similar, we reported only one picture as example.

DSC analysis can be used to determine the physical state of the lipid core in SLN (Müller et al., 2000; Mehnert and Mäeder, 2001), as the melting peak of the lipid core occurs at a lower temperature than that of the bulk lipid, mainly due to the nanocrystalline size of the lipids in the SLN (Westesen and Bunjees, 1995). The experiments performed to assess the physical state of the lipid core were carried out on unloaded SLN. While the calorimetric curve of CP bulk was characterized by a broad peak at about 39 °C and a main peak at about 50.5 °C, the calorimetric curve of unloaded SLN exhibited a well defined peak at about 38 °C and a shoulder at 42 °C (data not shown). The melting peak of these SLN, observed at a temperature about 12 °C lower than the bulk CP, indicated that the lipid

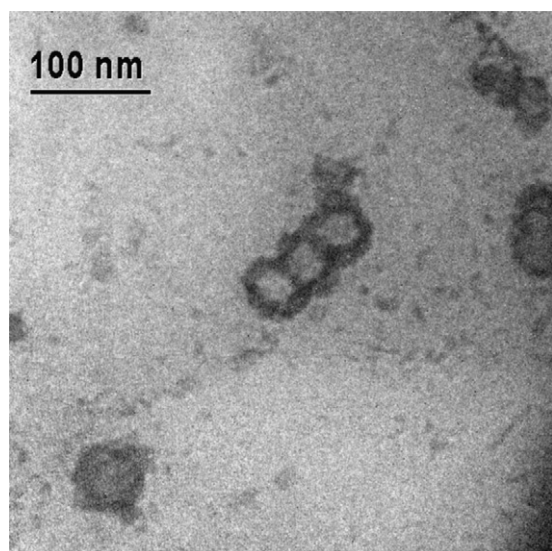


Fig. 2. TEM picture of SLN prepared by the PIT method. This image was obtained from SLN C1.

located in the core of the SLN was solid, thus confirming that solid lipid nanoparticles were prepared (Lee et al., 2007).

All the formulations tested showed pH values ranging from 4.78 to 5.10 (data not shown), a mean particle diameter in the range of 30–49 nm, and a single peak in size distribution (Table 2). When SLN formulations were clear, IDE was supposed to be completely incorporated into the SLN because being IDE poorly water soluble (3 µg/ml) if it had not loaded into SLN it would have given rise to a turbid system and/or a precipitate, as reported for other lipophilic drugs loaded into SLN (Jenning et al., 2000). Therefore, the loading capacity was determined as the maximum amount of IDE that could be loaded into SLN leading to a clear vehicle with no sign of precipitation.

As shown in Table 1, IDE loading capacity was lower (0.7%, w/w) for SLN prepared using isoceteth-20 as primary surfactant. The structure of the acyl chain of this surfactant could be responsible for the lower loading capacity since its isopropyl group could determine a steric hindrance, which prevented a higher drug loading.

When incorporating 1.1% (w/w) IDE into SLN prepared using ceteth-20 (SLN C) a decrease of SLN particle size was observed, while no significant particle size changes were observed by loading different amount of IDE to SLN I or SLN O (Table 2). A different status of IDE into the SLN core could be supposed depending on its concentration into the particles. Previous studies on SLN loaded with a compound analogous to IDE (coenzyme Q₁₀) pointed out that this active agent was in part homogeneously dispersed within the SLN matrix and in part arranged in separate nanoaggregates (Wissing et al., 2004). Therefore, different interactions between IDE and the surfactant layer could be expected depending on surfactant

Table 2

Characterization of IDE-loaded SLN: phase inversion temperature values (PIT), particle size (size ± S.D.), and polydispersity indexes ± S.D. (Poly ± S.D.) 24 h after their preparation.

SLN	PIT (°C)	Size ± S.D. (nm)	Poly ± S.D.
C1	80	48.7 ± 0.9	0.323 ± 0.019
C2	80	45.3 ± 1.1	0.289 ± 0.084
C3	81	29.9 ± 0.2	0.156 ± 0.017
I1	80	42.5 ± 0.6	0.291 ± 0.011
I2	80	45.4 ± 2.0	0.233 ± 0.027
O1	85	34.8 ± 0.1	0.161 ± 0.020
O2	84	36.1 ± 0.3	0.177 ± 0.123
O3	84	33.3 ± 0.1	0.140 ± 0.013

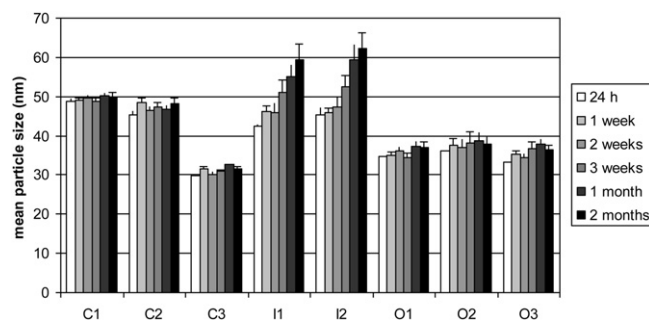


Fig. 3. Particle size of IDE-loaded SLN during storage at R.T. for 2 months.

lipophilicity and/or structure and IDE status. The lipophilicity of the surfactants used to prepare the SLN under investigation, expressed as hydrophilic lipophilic balance (HLB), were as follows: oleth-20 15.3, isoceteth-20 15.5, ceteth-20 15.7 and their chemical structure was different as isoceteth-20 has a branched acyl chain while oleth-20 and ceteth-20 have linear acyl chains, unsaturated and saturated respectively. Due to these surfactant properties, a different packing of the surfactant and co-surfactant molecules at the interface could be expected. As IDE is a lipophilic drug (LogP 3.49, calculated using Advanced Chemistry Development Software Solaris V. 4.67), the hydrophobic interactions that could occur between IDE and surfactant at the interfacial layer could affect particle curvature radius at different extent depending on its ability to penetrate the tail group region of the surfactant layer. Although a lower IDE interaction with the least lipophilic surfactants (ceteth-20) could be expected, our results showed a decrease of particle size upon addition of the highest percentage of IDE to SLN C, thus suggesting that in our experiments the structure of the surfactant may play an important role in determining drug/surfactant layer interactions. Further DSC studies are ongoing to better understanding the interactions between IDE and surfactant layer and drug state of dispersion within the lipid matrix.

As reported in the literature (Izquierdo et al., 2005), the HLB temperature (or PIT) is predictive of emulsion-based system stability: the higher the PIT, the greater the formulation stability. Since our SLN showed similar PIT values (Table 2), the same stability would have been expected for all IDE-loaded SLN. However, particle size analyses of formulations stored for 2 months at room temperature showed a different behavior for SLN I whose stability was lower compared to SLN C and SLN O (Fig. 3). This finding could be attributed to the structure of the surfactant used to prepare these SLN: a lower intercalation of IDE between the tail group region of the surfactant layer could occur owing to the branched acyl chain of this surfactant with a resulting looser packing of the surfactant layer that would increase aggregation phenomena. Experimental data showed less stability in terms of particle size for all the formulations when stored at 37 °C (data not shown). Less stability at higher temperature could be attributed to the introduction of energy into the system, that leads to particle growth and subsequent aggregation (Mehnert and Mäeder, 2001).

3.2. *In vitro* drug release

Since an essential requisite for a topical formulation to be effective is its ability to release the incorporated drug at a suitable rate and extent, preliminary *in vitro* release studies were carried out to assess IDE release from the SLN under investigation. IDE release was supposed to occur only from the lipid phase of SLN dispersion because of the poor water solubility of this drug that prevented its solution in water, as reported for other lipophilic drugs loaded into SLN (Jenning et al., 2000).

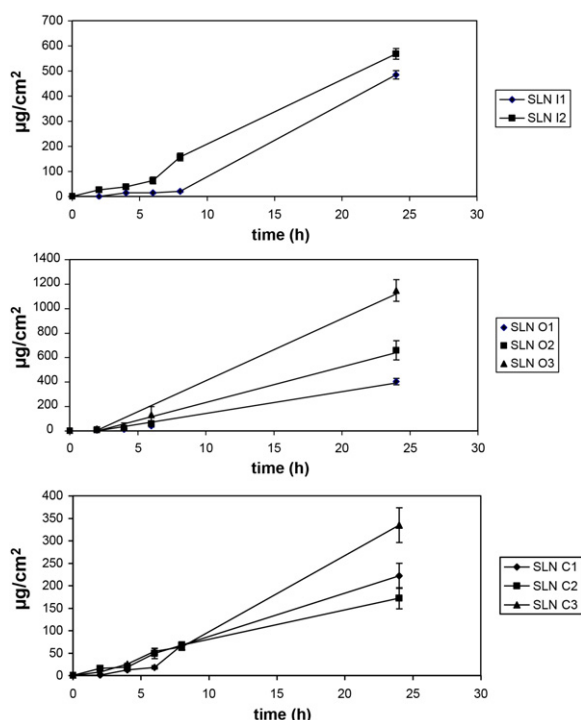


Fig. 4. *In vitro* release of IDE through cellulose membranes from IDE-loaded SLN: (a) SLN C1–3; (b) SLN I1–I2; (c) SLN O1–O3.

The infinite dose technique was used to evaluate *in vitro* IDE release from SLN by applying a large amount of formulation (200 µl) on the membrane surface. The use of an infinite dosing avoids drug depletion from the donor compartment during the experiment, thus ensuring a constant driving force for the release process and allowing the achievement of steady-state conditions.

Plotting the cumulative amount of active compound released during 24 h from SLN C, I and O as a function of time, different release profiles depending on type of surfactant and drug content were obtained (Fig. 4). An initial slow release followed by a faster release of the active compound was observed for all the SLN under investigation. A similar trend was reported by Jennings et al. (2000) who, studying *in vitro* release of vitamin A from SLN, attributed this pattern of release to the experimental conditions used during the study. When *in vitro* release experiments are performed leaving the donor phase open to the air (non-occlusion conditions), water evaporates from the SLN formulations, so that during 24 h the liquid dispersion turns slowly into a semisolid gel. This change of SLN from liquid dispersion into semisolid gel could be correlated with polymorphic transitions of the lipid matrix that could affect drug release from SLN, due to their different ability to include host molecule. Since IDE is poorly soluble in water, an increase of its release from SLN results in an increase of its thermodynamic activity that, in turn, increases its diffusion rate from the donor phase.

As shown in Fig. 4, comparing IDE release from SLN showing the same drug loading, the cumulative amount of IDE released after 24 h from SLN C was lower than that released from SLN I and O. The highest IDE release after 24 h was observed from SLN O loading IDE 1.1% (w/w) while SLN I and O provided similar amounts of IDE released when loading the same amount of drug. Since all the SLN showed similar particle size and the surfactant used had similar lipophilicity, the lower release of IDE from SLN C could be due to the different structure of the surfactant used to prepare these SLN. Since SLN C contained ceteth-20 as surfactant, its linear chain could determine a closer packing of the surfactant layer at the interface, resulting in a slower release of the loaded drug. This hypothesis

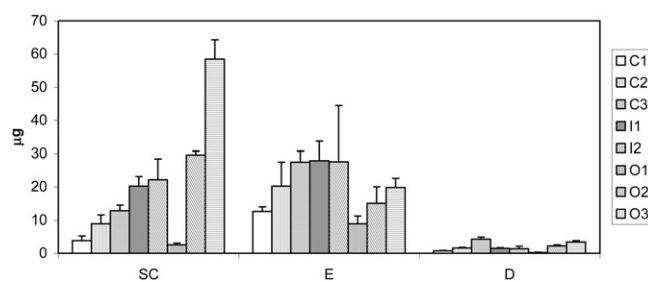


Fig. 5. *In vitro* skin penetration of IDE from IDE-loaded SLN. SC: stratum corneum; E: epidermis; D: dermis.

is supported by previous studies (Siekman and Westesen, 1996; Trotta, 1999) that highlighted the important role of interface structure in determining the barrier properties to drug diffusion out of O/W micelles.

3.3. *In vitro* skin permeation/penetration

In vitro skin permeation/penetration experiments were performed on new born pig skin since previous studies have shown that this animal model provided reliable information enabling to predict drug ability to permeate human skin. Indeed, pig stratum corneum is similar to human stratum corneum in terms of lipid composition, but it shows differences in terms of thickness. The thickness of new born pig stratum corneum, considerably thinner than that of adult pig, is more similar to that of human skin (Songkro et al., 2003; Cilurzo et al., 2007).

In our experiments, we did not use a control vehicle, such as creams or nanonemulsions, because different vehicles have different solubilizing properties and IDE thermodynamic activity would be different, making unreliable every comparison between IDE *in vitro* skin permeation results from control vehicle and IDE loaded SLN. Furthermore, recent studies (Li and Ge, 2012) demonstrated that IDE was able to permeate the skin using nanostructured lipid carriers, nanoemulsions or oils as vehicles and its permeation depended on vehicle composition.

As shown in Fig. 5, the amount of IDE penetrated into the different skin layers depended on IDE loading into the SLN and on the type of surfactant used while no IDE skin permeation occurred from all the SLN under investigation since IDE was not detected in the receptor fluid up to the end of the experiments. Other authors, studying SLN for isotretinoin targeting to the skin reported that SLN formulations avoided drug permeation through the skin, providing isotretinoin accumulation into the skin layers (Liu et al., 2007). In our studies, the highest IDE content was found in the epidermis when SLN containing ceteth-20 or isoceteth-20 as surfactant were applied on the skin while IDE distribution into the upper skin layers depended on the amount of IDE loaded when oleth-20 was used as surfactant.

Applying on the skin surface SLN C1, C2 or C3, the amount of IDE penetrated into the stratum corneum was lower than that observed in the epidermis and the drug content in these skin layers increased by increasing the percentage of IDE loaded into the SLN. As for SLN I1 and I2, the amount of IDE penetrated into the horny layer and the epidermis was similar, regardless of the amount of drug loaded. A different trend was observed when SLN O1, O2 or O3 were tested: SLN O1, loading the lowest amount of IDE (0.5%, w/w), provided a concentration of IDE higher in the epidermis than in the stratum corneum while SLN O2 and SLN O3 gave rise to IDE accumulation in the stratum corneum rather than in the epidermis.

The results of these experiments suggest that, apart from SLN interactions with the skin, IDE release from the nanoparticles could play an important role in determining IDE distribution into the

skin layers as well. The comparison of *in vitro* release results with skin penetration data pointed out that IDE skin penetration from all the SLN was not limited by its release from the vehicle since, for each SLN tested, the cumulative amount of IDE released after 24 h was much higher than the cumulative amount of IDE penetrated after 24 h in all the skin layers. However, the amount of drug released seemed to affect IDE distribution into the stratum corneum and the epidermis. As shown in Fig. 5, SLN C1–3, SLN I1 and I2 and SLN O1, that released a cumulative amount of IDE ranging from 170 to 570 $\mu\text{g}/\text{cm}^2$ after 24 h provided an IDE accumulation into the epidermis. Although SLN O2 released an amount of IDE in the same range, IDE accumulated in the stratum corneum rather than in epidermis. When SLN O3, that provided the highest IDE release after 24 h, was applied on the skin surface, IDE content into the horny layer was three-fold higher than that found in the epidermis. These data suggest that a great amount of IDE released from the SLN could form a reservoir into the stratum corneum from which the drug slowly diffused out into the underlying epidermis. On the contrary, when lower amount of IDE were released, SLN interactions with the horny layer could outweigh the effect of drug release on skin penetration, thus determining an IDE accumulation in the stratum corneum or in the epidermis, depending SLN ability to interact with the skin components. Therefore, further studies are ongoing to elucidate the mechanism of IDE loaded interactions with biomembrane in order to evaluate the key parameters in determining IDE distribution into the different skin layers.

4. Conclusion

Studying *in vitro* skin permeation and penetration of IDE from SLN loading different amount of IDE and containing different non-ionic surfactants, we evidenced that no IDE permeation occurred while IDE penetration into the different skin layers depended on both drug loading into the SLN and SLN composition. It is interesting to note that, using the SLN under investigation, IDE accumulated in the upper skin layers, *i.e.* stratum corneum and epidermis. The results of our *in vitro* skin permeation and penetration studies suggest that loading IDE into suitable SLN could provide a useful tool to achieve IDE targeting to the upper skin layers and to improve IDE bioavailability after topical administration.

References

- Bernard, E., Dubois, J.L., Wepierre, J., 1997. Importance of sebaceous glands in cutaneous penetration of an antiandrogen: target effect of liposomes. *J. Pharm. Sci.* 86, 573–578.
- Cilurzo, F., Minghetti, P., Sinico, C., 2007. Newborn pig skin as model membrane in *in vitro* drug permeation studies: a technical note. *AAPS Pharm. Sci. Technol.* 8, E94.
- Crane, F.L., 2001. Biochemical functions of coenzyme Q10. *J. Am. Coll. Nutr.* 20, 591–598.
- Dallner, G., Sindelar, P.J., 2000. Regulation of ubiquinone metabolism. *Free Radic. Biol. Med.* 29, 285–294.
- Dreher, F., Maibach, H.I., 2001. Protective effects of topical antioxidants in humans. *Curr. Probl. Dermatol.* 29, 157–164.
- Friend, D.R., 1992. *In vitro* skin permeation techniques. *J. Control. Release* 18, 235–248.
- Hoppe, U., Bergemann, J., Diembeck, W., Ennen, J., Gohla, S., Harris, I., Jacob, J., Kielholz, J., Mei, W., Pollet, D., Schachtschabel, D., Sauer mann, G., Schreiner, V., Stüb, F., Steckel, F., 1999. Coenzyme Q₁₀, a cutaneous antioxidant and energizer. *Biofactors* 9, 371–378.
- Imada, I., Fujita, T., Sugiyama, Y., Okamoto, K., Kobayashi, Y., 1989. Effects of idebenone and related compounds on respiratory activities of brain mitochondria, and on lipid peroxidation of their membranes. *Arch. Gerontol. Geriatr.* 8, 323–341.
- Izquierdo, P., Feng, J., Esquena, J., Tadros, T.F., Dederen, J.C., Garcia, M.J., Azemar, N., Solans, C., 2005. The influence of surfactant mixing ratio on nano-emulsion formation by the PIT method. *J. Colloid Interface Sci.* 285, 388–394.
- Jenning, V., Schäfer-Korting, M., Cohn, S., 2000. Vitamin A-loaded solid lipid nanoparticles for topical use: drug release properties. *J. Control. Release* 66, 115–126.
- Junyaprasert, V.B., Teeranachaideekul, V., Souto, E.B., Boonme, P., Müller, R.H., 2009. Q10-loaded NLC versus nanoemulsions: stability, rheology and *in vitro* skin permeation. *Int. J. Pharm.* 377, 207–214.
- Lee, M.K., Lim, S.J., Kim, C.K., 2007. Preparation, characterization and *in vitro* cytotoxicity of paclitaxel loaded sterically stabilized solid lipid nanoparticles. *Biomaterials* 28, 2137–2146.
- Li, B., Ge, Z.Q., 2012. Nanostructured lipid carriers improve skin permeation and chemical stability of idebenone. *AAPS Pharm. Sci. Technol.* 13, 276–283.
- Liu, J., Hu, W., Chen, H., Ni, Q., Xu, H., Yang, X., 2007. Isotretinoin-loaded solid lipid nanoparticles with skin targeting for topical delivery. *Int. J. Pharm.* 328, 191–195.
- Lukowski, G., Kasbohm, J., Pfliegel, P., Illing, A., Wulff, H., 2000. Crystallographic investigation of cetyl palmitate solid lipid nanoparticles. *Int. J. Pharm.* 196, 201–205.
- Mehnert, W., Mäeder, K., 2001. Solid lipid nanoparticles. Production, characterization and applications. *Adv. Drug Deliv. Rev.* 47, 165–196.
- Mezei, M., Touitou, E., Junginger, H.E., Weiner, N.D., Tagai, T., 1994. Liposomes as carriers for topical and transdermal delivery. *J. Pharm. Sci.* 9, 1189–1203.
- Montenegro, L., Trapani, A., Latrofa, A., Puglisi, G., 2012. *In vitro* evaluation on a model of blood brain barrier of idebenone-loaded solid lipid nanoparticles. *J. Nanosci. Nanotechnol.* 12, 330–337.
- Montenegro, L., Campisi, A., Sarpietro, M.G., Carbone, C., Acquaviva, R., Raciti, G., Puglisi, G., 2011. *In vitro* evaluation of idebenone-loaded solid lipid nanoparticles for drug delivery to the brain. *Drug Dev. Ind. Pharm.* 37, 737–746.
- Müller, R.H., Mäeder, K., Gohla, S., 2000. Solid lipid nanoparticles (SLN) for controlled drug delivery: a review of the state of the art. *Eur. J. Pharm. Biopharm.* 50, 161–177.
- Papakostas, D., Rancan, F., Sterry, W., Blume-Peytavi, U., Vogt, A., 2011. Nanoparticles in dermatology. *Arch. Dermatol. Res.* 303, 533–550.
- Pardeike, J., Hommoss, A., Müller, R.H., 2009. Lipid nanoparticles (SLN, NLC) in cosmetic and pharmaceutical dermal products. *Int. J. Pharm.* 366, 170–184.
- Schols, L., Meyer, C.H., Schmid, G., Wihelms, I., Przuntek, H., 2004. Therapeutic strategies in Friedreich's ataxia. *J. Neural Transm. Suppl.* 68, 135–145.
- Shah, V.P., Elkins, J., Lam, S.Y., Skelly, J.P., 1989. Determination of *in vitro* drug release from hydrocortisone creams. *Int. J. Pharm.* 53, 53–59.
- Siekman, B., Westesen, K., 1996. Investigations on solid lipid nanoparticles prepared by precipitation in o/w emulsions. *Eur. J. Pharm. Biopharm.* 43, 104–109.
- Sies, H., 1985. Introductory remark. In: Sies, H. (Ed.), *Oxidative Stress*. Academic Press, Orlando, pp. 1–7.
- Songkro, S., Purwo, Y., Becket, G., Rades, T., 2003. Investigation of newborn pig skin as an *in vitro* animal model for transdermal drug delivery. *STP Pharm. Sci.* 13, 133–139.
- Thiele, J.J., Dreher, F., Packer, L., 2000. Antioxidant defence systems in skin. In: Elsner, P., Maibach, H., Rougier, A. (Eds.), *Drugs in Cosmetic: Cosmeceuticals?* Dekker, New York, pp. 145–187.
- Thiele, J.J., Traber, M.G., Packer, L., 1998. Depletion of human stratum corneum vitamin E: an early and sensitive *in vivo* marker of UV-induced photooxidation. *J. Invest. Dermatol.* 110, 756–761.
- Trotta, M., 1999. Influence of phase transformation on indomethacin release from microemulsions. *J. Control. Release* 60, 399–405.
- Wang, J.-J., Liu, K.-S., Sung, K.C., Tsai, C.-Y., Fang, J.-Y., 2009. Lipid nanoparticles with different oil/fatty ester ratios as carriers of buprenorphine and its prodrugs for injection. *Eur. J. Pharm. Sci.* 38, 138–146.
- Westesen, K., Bunjees, H., 1995. Do nanoparticles prepared from lipids solid at room temperature always possess a solid lipid matrix? *Int. J. Pharm.* 115, 129–131.
- Wieland, E., Schutz, E., Armstrong, V.W., Kuthe, F., Heller, C., Oellerich, M., 1995. Idebenone protects hepatic microsomes against oxygen radical-mediated damage in organ preservation solutions. *Transplantation* 60, 444–451.
- Wissing, S.A., Müller, R.H., Manthei, L., Mayer, C., 2004. Structural characterization of Q10-loaded solid lipid nanoparticles by NMR spectroscopy. *Pharm. Res.* 21, 400–405.
- Zhang, J., Smith, E., 2011. Percutaneous permeation of betamethasone 17-valerate incorporated in lipid nanoparticles. *J. Pharm. Sci.* 100, 896–903.